

# 針狀太陽熱集熱器의 性能과 傳熱特性에 關한 研究

서 정 윤\* , 박 남 세\*\*

A Study on Performance And Heat Transfer Characteristics  
of Spine Fin Tube Solar Collector.

Jeong Yun Seo\* , Nam Sai Park\*\*

## 抄 錄

이 研究는 기존의 平板集熱器와 그 型狀이 다른 Spine fin (針狀) tube 태양열집열기를 製作 使用하여 理論과 實驗을 통해 그 性能과 熱傳達 特性을 규명하고 다른 平板集熱器와 比較하므로써 Spine fin tube 集熱器의 適用可能性을 제시하였다.

또한 이 集열기의 最適 使用條件과 그 設計因子들이 제시되었다.

---

\* 正會員, 仁荷大學校 工科大學

\*\* 仁荷大學校 大學院

**Nomenclatures**

$A_c$ : Collector area $m^2$	$T_{o1}$ : Mean tube temperature of front side with spine fin $^{\circ}C$
$C_p$ : Specific heat of fluid $Kcal/kg^{\circ}C$	$T_{o2}$ : Mean tube temperature of back side with spine fin $^{\circ}C$
$d_1$ : Outside diameter of spine fin tube m.	$T_t$ : Skin temperature of tube $^{\circ}C$
$d_2$ : Outside diameter of copper tube m.	$T_{t1}$ : Mean tube temperature of front side without fin $^{\circ}C$
$d_3$ : Inside diameter of copper tube m.	$T_{t2}$ : Mean tube temperature of back side without fin $^{\circ}C$
$G$ : Mass flow rate $l/min m^2$ .	$T_{tm}$ : Mean tube temperature without fin $^{\circ}C$
$h_1$ : Heat loss coefficient of front side of collector $Kcal/m^2 h^{\circ}C$	$T_{out1}$ : Outlet temperature with spine fin $^{\circ}C$
$h_2$ : Heat loss coefficient of back side of collector $Kcal/m^2 h^{\circ}C$	$T_{out2}$ : Outlet temperature without fin $^{\circ}C$
$h_3$ : Heat transfer coefficient of fluid $Kcal/m^2 h^{\circ}C$	$U_l$ : Collector overall heat loss $Kcal/m^2 h^{\circ}C$
$I$ : Rate of solar insolation $Kcal/m^2 h$	$y$ : Correction factor
$K_1$ : Thermal conductivity of aluminum $Kcal/m h^{\circ}C$	
$K_2$ : Thermal conductivity of copper $Kcal/mh^{\circ}C$	
$l$ : Fin length m.	
$\dot{m}$ : Mass flow rate $kg/s$	
$t$ : Fin thickness for circular direction m.	
$T_a$ : Ambient temperature $^{\circ}C$	
$T_{in}$ : Inlet temperature $^{\circ}C$	
$T_f$ : Local fluid temperature $^{\circ}C$	
$T_{fm}$ : Local mean tube temperature with spine fin $^{\circ}C$	
$T_p$ : Local fin temperature $^{\circ}C$	
$T_{pm}$ : Mean fin temperature $^{\circ}C$	
$T_{pm1}$ : Local fin temperature of front side varying with circular angle $^{\circ}C$	
$T_{pm2}$ : Mean fin temperature of back side $^{\circ}C$	
$T_{pm3}$ : Mean fin temperature of front side $^{\circ}C$	
$T_o$ : Contact temperature of fin and tube $^{\circ}C$	
	<b>Greek letters</b>
	$\alpha$ : Absorptance of blackened fin and tube
	$\beta$ : Concentration factor of fin
	$\tau$ : Transmittance of cover-glass
	$\theta$ : Circular angle of tube (deg)
	$\theta_o$ : Incident angle of solar radiation (deg)

**1. Introduction**

Various types and special surface treatment for solar collecting appliance have been researched to enhance its efficiency and the Flat plate solar collector has been a major object due to its advantageous fabrication, installation and maintenance.<sup>4) 5) 6) 7)</sup>

YOKOTA et al<sup>1)</sup> investigated the theoretical analysis and experimental measurement on roll-bond type flat plate solar collector.

And this study evaluated the correlations 0.5mm thick.

for absorber plate thickness and collector pitch.

This study is aimed to search the heat transfer characteristics and performances of spine fin tube solar collector ( usually used for evaporator and condenser on commercial air-conditioner ).

The predicted effects by the spine fin tube solar collector are as follow.

1) Surface absorptance of solar radiation will be higher than the flat plate solar collector resulting from the much reflectance of solar ray attached by radial fins around the spine fin tube as show in Fig 1-1, Fig1-2.

2) Though the insolation rate would be changed with incident angle on the flat plate collector, the rate of spine fin tube solar collector is scarcely changed.

3) As the convection is restrained through the trapped air layer between the fins the collector heat loss could be reduced.

While these advantages are predicted, the collector air packing between the cover-glass and absorber surface must be maintained highly lest water should infiltrate the substrate of aluminum fins and copper tube because of electric-corrosion.

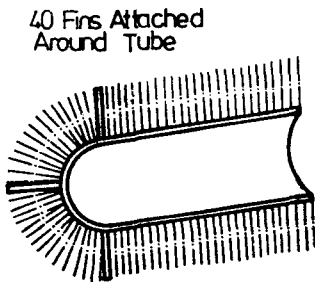


Fig. 1.1 Longitudinal cross section of spine fin tube

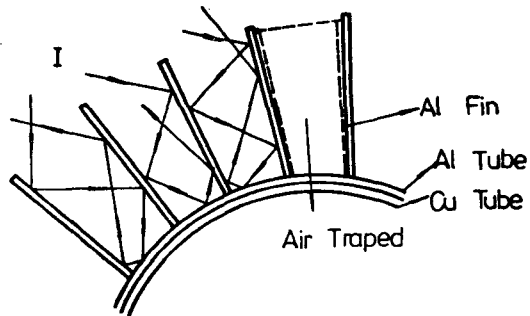


Fig. 1.2 Reflection of insolation on the fin element

## 2. Theoretical Analysis

### 2-1 Conduction of fin

Heat transfer phenomena of the spine fin tube solar collector is shown in Fig 2-1.

Energy balance on an element of the fin thickness  $dx$  as shown in Fig 2-2.

$$q_x + q_f - q_{x+dx} = 0 \dots\dots\dots(1)$$

$$q_x = -k_1 t \frac{dT_p}{dx}$$

$$q_{x+dx} = -k_1 t \frac{d}{dx} (T_p + \frac{dT_p}{dx} dx)$$

$$q_f = [ (\tau \alpha) I \cos \theta - U_l (T_p - T_a) ] dx$$

Thus we get following equation

$$\frac{d^2 \Phi}{dx^2} - m^2 \Phi = 0 \dots\dots\dots(2)$$

where  $m^2 = U_l / k_1 t$ ,

$$\Phi = T_p - [ T_a + \frac{(\tau \alpha) I \cos \theta}{U_l} ]$$

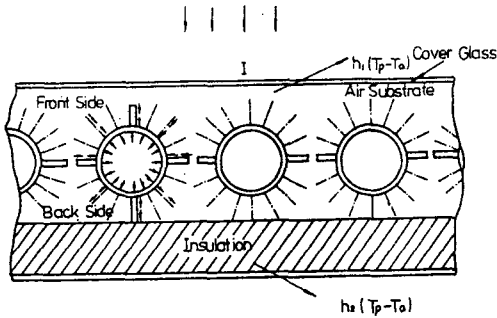


Fig. 2.1 Heat transfer behaviors of solar collector

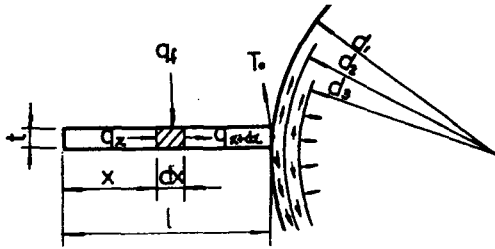


Fig. 2.2 Conduction of fin element

The solution with boundary condition

$$\frac{dT_p}{dx} = 0 \text{ at } x=0, T_p = T_a \text{ at } x=l$$

is

$$T_p = T_a \frac{\cosh(mx)}{\cosh(ml)} + \left[ T_a + \frac{(\tau\alpha)I}{U_1} \cos\theta \right] \times \left[ 1 - \frac{\cosh(mx)}{\cosh(ml)} \right] \dots\dots\dots (3)$$

Mean fin temperature  $T_{pm1}$  at the front side may be obtained by  $U_1 = h_1$  in equation

$$T_{pm1} = \int_0^l T_p dx / \int_0^l dx = T_a \eta_f + (1 - \eta_f) \left[ T_a + \frac{(\tau\alpha)I}{h_1} \cos\theta \right] \dots\dots\dots (4)$$

where,  $\eta_f = \tanh(ml) / (ml)$  called fin efficiency.

At back side of collector, no insolation is received and mean fin temperature  $T_{pm2}$  is obtainable by  $I=0$  in equation (4)

$$T_{pm2} = T_a \eta_f + (1 - \eta_f) T_a \dots\dots\dots (5)$$

Since  $T_{pm1}$  is varying with circular angle  $\theta$ ,  $T_{pm1}$  must be integrated by  $\theta$  and

rewritten

$$T_{pm3} = \frac{2}{\pi} \int_0^{\pi/2} T_{pm1} d\theta = T_a \eta_f + (1 - \eta_f) \left[ T_a + \frac{2(\tau\alpha)I}{h_1 \pi} \right] \dots\dots (6)$$

Thus the mean fin temperature  $T_{pm}$  at the longitudinal arbitrary cross section becomes

$$T_{pm} = \frac{1}{2} (T_{pm2} + T_{pm3}) = T_a \eta_f + (1 - \eta_f) \left[ T_a + \frac{(\tau\alpha)I}{h_1 \pi} \right] \dots\dots\dots (7)$$

### 2-2 Contact temperature $T_o$ and mean tube temperature $T_{fm}, T_{tm}$

1) For the case with spine fin

Energy balance on an element of differential volume in Fig.2-3, we consider the radial heat flow only for the unit depth of tube length.

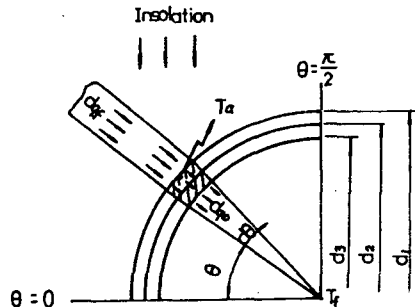


Fig.2.3 Conduction phenomena of fin tube element for differential volume (dashed line)

$$dq_f = dq_w \dots\dots\dots (8)$$

$dq_f$  is obtainable from equation(3)

$$dq_f = k_1 t \frac{d_1}{2} d\theta \frac{dT_p}{dx} \Big|_{x=l} = \frac{d_1 \ell \eta_f}{2t} \left[ (\tau\alpha)I \cos\theta - U_1 (T_o - T_a) \right] d\theta \dots\dots\dots (9)$$

And  $dq_w$  is expressed from the thermal resistance

$$dq_w = \frac{T_o - T_f}{\frac{\ell_n(r_1/r_2)}{k_1 d\theta} + \frac{\ell_n(r_2/r_3)}{k_2 d\theta} + \frac{1}{\frac{1}{2} h_3 d_3 d\theta}} \dots (10)$$

Let the denominator of equation (10) as  $a_1$  and after some arrangement, contact term-perature  $T_o$  is obtained

$$T_o = \frac{a_1 d_1 \ell \eta_f [(\tau\alpha)I \cos\theta + h_1 T_o] + 2t T_f}{2t + a_1 d_1 \ell \eta_f h_1} \dots (11)$$

And because  $T_o$  varies with circular angle  $\theta$ , the mean tube temperature  $T_{o1}$  becomes

$$T_{o1} = \frac{2}{\pi} \int_0^{\frac{\pi}{2}} T_o d\theta$$

$$= \frac{a_1 d_1 \ell \eta_f [ \frac{2}{\pi} (\tau\alpha)I + h_1 T_o ] + 2t T_f}{2t + a_1 d_1 \ell \eta_f h_1} \dots (12)$$

For the back side, the mean tube temperature  $T_{o2}$  become by  $I=0$  and  $h_1=h_2$  in equation (12)

$$T_{o2} = \frac{a_1 d_1 \ell \eta_f h_2 T_o + 2t T_f}{2t + a_1 d_1 \ell \eta_f h_2} \dots (13)$$

Accordingly at the longitudinal arbitrary section, the mean tube temperature  $T_{fm}$  is

$$T_{fm} = \frac{1}{2} (T_{o1} + T_{o2})$$

$$= \frac{1}{2} (A + C) + \frac{(B + D)}{2} T_f \dots (14)$$

where,

$$A = \frac{a_1 d_1 \ell \eta_f [ \frac{2}{\pi} (\tau\alpha)I + h_1 T_o ]}{2t + a_1 d_1 \ell \eta_f h_1},$$

$$B = \frac{2t}{2t + a_1 d_1 \ell \eta_f h_1}$$

$$C = \frac{a_1 d_1 \ell \eta_f h_2 T_o}{2t + a_1 d_1 \ell \eta_f h_2}, \quad D = \frac{2t}{2t + a_1 d_1 \ell \eta_f h_2}$$

2) For the case of tube only

Considering on energy balance for the

$$\text{differential volme, } dq_t = dq_w \dots (15)$$

Where,  $dq_t$ ; energy incoming,  $dq_w$ : energy transferring to the fluid From Fig

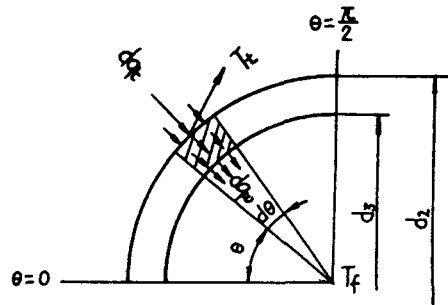


Fig. 2.4 Conduction phenomena of tube element for differential volume ( dashed line )

2-4,  $dq_t$  is expressed as

$$dq_t = [ (\tau\alpha)I \cos(\theta - \theta_0) - U_t (T_t - T_o) ] \times \frac{d_2}{2} d\theta \dots (16)$$

And  $dq_w$  is obtained in same manner of previous case

$$dq_w = \frac{T_t - T_f}{\frac{\ln(r_2/r_3)}{k_2 d\theta} + \frac{1}{h_3 (\frac{d_3}{2}) d\theta}} \dots (17)$$

let the denominator of equation (17) as  $a_2$ .

Assuming the incident angle  $\theta_0 = \frac{\pi}{2}$ , the

local tube temperature on the front side

would be written by making  $U_t = h_1$

$$T_t = \frac{a_2 d_2 [ (\tau\alpha)I \cos(\theta - \frac{\pi}{2}) + h_1 T_o ] + 2T_f}{2 + a_2 d_2 h_1} \dots (18)$$

Thus the mean tube temperature  $T_{t1}$  on the front side becomes

$$T_{t1} = \frac{2}{\pi} \int_0^{\frac{\pi}{2}} T_t d\theta$$

$$= \frac{a_2 d_2 [ \frac{2}{\pi} (\tau\alpha)I + h_1 T_o ] + 2T_f}{2 + a_2 d_2 h_1} \dots (19)$$

For the back side the mean tube temper-

ature  $T_{i2}$  is obtained by replacing  $I=0$  and  $h_1=h_2$  in equation (19)

$$T_{i2} = \frac{a_2 d_2 h_2 T_a + 2T_f}{2 + a_2 d_2 h_2} \dots\dots\dots (20)$$

Accordingly, the tube temperature at the longitudinal arbitrary section is expressed as

$$T_{tm} = \frac{1}{2}(T_{i1} + T_{i2}) = \frac{1}{2}(E+G) + \frac{(H+F)}{2} T_f \dots\dots\dots (21)$$

Where,  $E = \frac{a_2 d_2 [ \frac{2}{\pi} (\tau\alpha) I + h_1 T_a ]}{2 + a_2 d_2 h_1}$   
 $G = \frac{a_2 d_2 h_2 T_a}{2 + a_2 d_2 h_2}$ ,  $F = \frac{2}{2 + a_2 d_2 h_1}$   
 $H = \frac{2}{2 + a_2 d_2 h_2}$

### 2-3 Outlet temperature of collector

Assuming  $dQ_f$  inflowing energy per unit time and  $dQ_f$  outflowing energy, the useful energy gain  $dQ_u$  becomes

$$dQ_u = dQ_f - dQ_f \dot{m} c_p (T_f + dT_f) - \dot{m} c_p T_f = \dot{m} c_p dT_f \dots\dots\dots (22)$$

useful energy gain  $dQ_u$  is sum of energy from the fin tube  $dQ_{fin}$  and the tube without fin  $dQ_{tube}$ .

$$dQ_u = dQ_{fin} + dQ_{tube} \dots\dots\dots (23)$$

1) Effective energy gain  $dQ_{fin}$  from the fin

Effective energy gain on the projected area of the spine fin tube at the front side is expressed as

$$dQ_{f1} = y\beta(2\ell + d_1) [ (\tau\alpha) I - h_1 (T_{pm} - T_a) ] dZ \dots\dots\dots (24)$$

where,  $y$ : correction factor,

$\beta$ : concentration factor of fin

$Z$ : unit length of tube

Calculated  $\beta=1$  in the case of 20 fins/inch of spine fin tube while  $\beta=0$  of without fins.

And for the back side of spine fin tube no insulation was assumed and exist heat radiation only from the fin

$$dQ_{f2} = -y\beta(2\ell + d_1) h_2 (T_{pm} - T_a) dZ \dots (25)$$

thus  $dQ_{fin} = dQ_{f1} + dQ_{f2}$   
 $= y\beta(2\ell + d_1) [ (\tau\alpha) I - U_l (T_{pm} - T_a) ] dZ \dots (26)$

2) Effective energy gain  $dQ_{tube}$  from the tube only.

From the projected area of the tube, effective energy gain is expressed as

$$dQ_{t1} = d_2(1-\beta) [ (\tau\alpha) I - h_1 (T_{tm} - T_a) ] dZ \dots\dots\dots (27)$$

For the back side,  $I=0$  and  $h_1=h_2$  is fitted.

$$dQ_{t2} = -d_2(1-\beta) h_2 (T_{tm} - T_a) \dots\dots\dots (28)$$

Thus,  $dQ_{tube} = dQ_{t1} + dQ_{t2}$   
 $= d_2(1-\beta) [ (\tau\alpha) I - U_l (T_{tm} - T_a) ] dZ \dots (29)$

From equation (22), (25), (28),  $dQ_u$  is arranged as

$$dQ_u = [ (2\ell + d_1) y\beta + d_2(1-\beta) [ (\tau\alpha) I + U_l T_a ] dZ - U_l ] (2\ell + d_1) y\beta \left\{ \frac{(A+C)}{2} + \frac{(B+D)}{2} T_f \right\} \eta_f + Y + d_2(1-\beta) \left\{ \frac{(E+G)}{2} + \frac{(H+F)}{2} T_f \right\} dZ \dots\dots\dots (30)$$

where,  $Y = (1 - \eta_f) \left[ T_a + \frac{(\tau\alpha) I}{h_1 \pi} \right]$

Equation (21), (29) is rearranged for about fluid temperature  $T_f$

$$\frac{dT_f}{dZ} + JT_f = K \dots\dots\dots (31)$$

where  $J = \frac{U_l}{2\dot{m}c_p} [ y\beta\eta_f(2\ell + d_1)(B+D) ]$

$$+ d_2 (1 - \beta) (H + F) ]$$

$$K = \frac{1}{\dot{m}c_p} [ y\beta(2\ell + d_1) + d_2 (1 - \beta) ] [ (\tau\alpha)I$$

$$+ U_l T_a ] - \frac{U_l}{2\dot{m}c_p} [ y\beta(2\ell + d_1) \{ (A + C) \cdot$$

$$\eta_f + 2Y \} + d_2 (1 - \beta) (E + G) ]$$

The solution of equation (30) with boundary condition  $T_f = T_{in}$  at  $Z=0$ ,  $T_f = T_{out}$  at  $Z=L$  is obtained

$$T_f = C_1 e^{-jz} + \frac{K}{j} \dots \dots \dots (32)$$

Outlet temperature is determined

$$T_{out1} = T_{in} e^{-jz} + \frac{K}{j} (1 - e^{-jz}) \Big|_{\beta=1} \dots (33)$$

$$T_{out2} = T_{in} e^{-jz} + \frac{K}{j} (1 - e^{-jz}) \Big|_{\beta=0} \dots (34)$$

**2-4 Collector efficiency  $\eta$**

Collector efficiency  $\eta$  is defined as<sup>(6)</sup>

$$\eta = \frac{Q_u / A_c}{1} = \frac{\dot{m}c_p (T_{out} - T_{in})}{A_c \cdot I} \dots \dots \dots (35)$$

where  $Q_u$  is calculated from temperature difference of inlet and outlet of the collector.

Hence the performance curve is drawn  $\eta$  in  $y$  coordinate and

$$\left[ \frac{(T_{out} + T_{in})}{2} - T_a \right] / I \text{ in } x \text{ coordinate.}$$

**2-5 Collector loss coefficient  $U_l$ <sup>(2)(3)</sup>**

Collector loss coefficient  $U_l$  is quoted by Willam Beckmans emperical formulas.<sup>(6)</sup>

$$U_l = h_1 + h_2$$

$$h_1 = \left[ \frac{\eta}{C/T_{pm} \left\{ \frac{T_{pm} - T_a}{(n+f)} \right\} e} + \frac{1}{h_w} \right]^{-1}$$

$$+ \frac{\sigma(T_{pm} + T_a)(T_{pm}^2 + T_a^2)}{(\epsilon_p + 0.00591 h_w)^{-1} + \frac{2n+f-1+0.133 \epsilon_p}{\epsilon_g} \frac{v}{n}}$$

$$\dots \dots \dots (36)$$

$$h_2 = \frac{K}{L} \dots \dots \dots (37)$$

- where  $n$  : number of cover - glass  
 $f$  :  $(1 + 0.089 h_w - 0.1166 h_w)$   
 $(1 + 0.07866n)$   
 $C$  :  $520 (1 - 0.000051\beta^2)$  for  $0^\circ < \beta$   
 $< 70^\circ$   
 $e$  :  $0.43 (1 - 100 / T_{pm})$   
 $\beta$  : collectors tilt angle (deg)  
 $\epsilon_g$  : emittance of cover-glass (0.88)  
 $\epsilon_p$  : emittance of absorber plate  
 (black paint 0.95)  
 $T_{pm}$  : mean temperature of absorber  
 (°K)  
 $h_w$  : wind factor ( $h_w = 5.7 + 3.8 v$ )  
 $v$  : wind velocity (m/s)

**2-6 Heat tranfer coefficient  $h_3$**

The coefficient of  $h_3$  was calculated as below along the fluid velocities of the tube inside.<sup>(8)</sup>

i) In laminar flow  
 $Nu = h_3 \cdot d_3 / K = 4.364 \dots \dots \dots (38)$

ii) In turbulent flow  
 $Nu = 0.023 Re^{0.8} Pr^{0.4} \dots \dots \dots (39)$

**3. Experiment**

**3-1 Experimental apparatus**

The experiment for this study was performed on May 2 to June 5 in 1983 through the preliminary experiment and collector

located to face due south 1.5m above the roof with tilted angle  $45^\circ$  as shown in Fig 3-1.

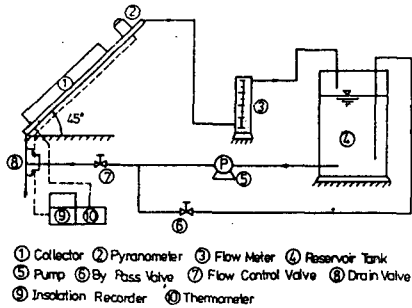


Fig. 3.1 Schematic diagram of experimental apparatus

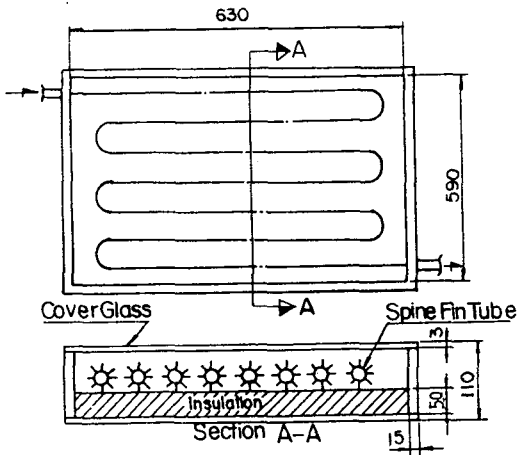


Fig. 3.2 Collector dimensions for experiment

### 3-2 Collector

Two collectors with a series copper tube and spine fin tube respectively were prepared for experiment and their surfaces were coated with acrylic black paint spray.

Each collector was consisted of 15mm thick board, 50mm glass-wool for insulation and 3mm thick common transparent glass for cover-glass.

Detailed specifications are illustrated in Fig 3-2 and Fig 3-3.

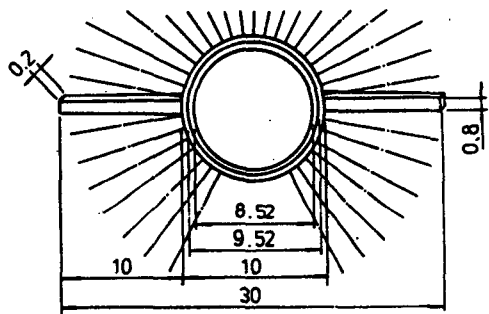


Fig. 3.3 Specification of spine fin

## 4. Discussion

In the case of tube collector without fin in Fig 4-1, the result showed average  $2^\circ\text{C}$  of temperature difference at the tube cross section for central part of collector  $\theta = 90^\circ$  and  $\theta = -90^\circ$  respectively, when the insolation rate reached over  $600\text{Kcal}/\text{m}^2\text{h}$  to  $800\text{Kcal}/\text{m}^2\text{h}$ , but it was almost same when the rate was below  $400\text{Kcal}/\text{m}^2\text{h}$ .

Similary in the spine fin tube collector in Fig 4-2, the temperature difference was resulted in average  $1^\circ\text{C}$  below.

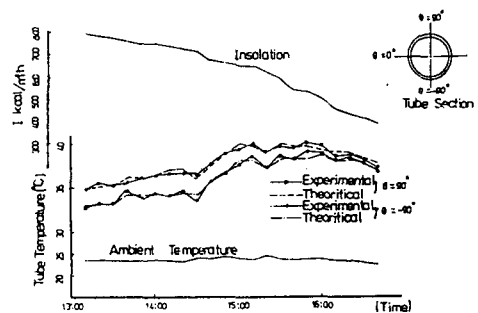


Fig4.1 Comparison of tube temperature to with no fin

This is notable that the circular heat flow around the spine fin tube is occurred well compared that of no fin tube because of fin effects as indicated in preceding



introduction.

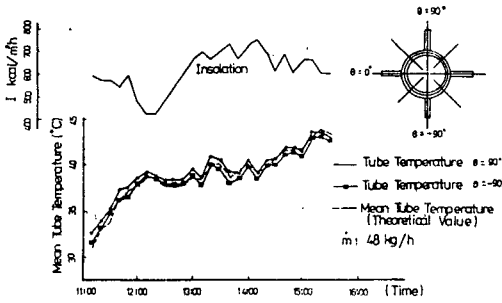


Fig. 4.2 Comparison of mean tube temperature  $T_{fm}$  with spine fin (at central part of collector)

Fig 4-3 represents inlet temperature, outlet temperature and insolation variations when mass flow rate equals 24kg/h with no fin tube collector.

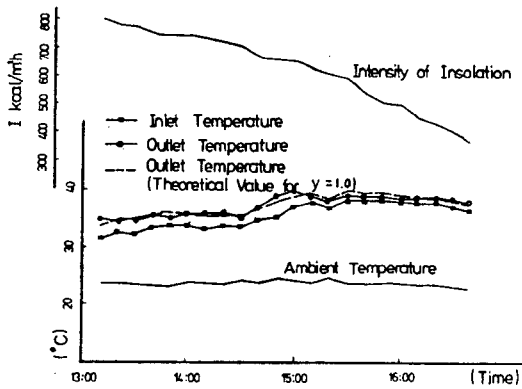


Fig. 4.3 Experimental results for no fin tube solar collector with  $G=1 \text{ l/min m}^2$

In Fig 4-4 plotted as Fig 4-3, when the correction factor  $y$  was 1.5 better agreement between the theoretical and experimental values was resulted rather than  $y$  was 1.0.

To find out the optimum flow rate range the outlet temperature variation was plotted in accordance with various theoretical flow rates as in Fig 4-5.

The figures 4-6 and 4-7 were presented to observe the correlations between the fin efficiency, length and thickness.

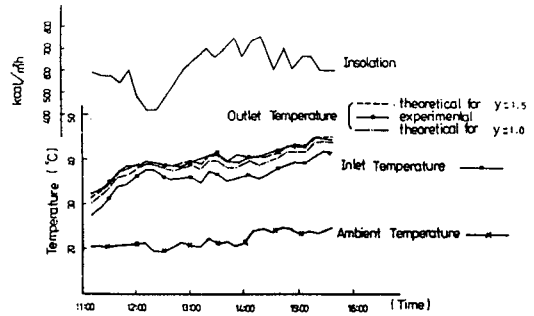


Fig. 4.4 Experimental results for spine fin tube solar collector with  $G=2.16 \text{ l/min m}^2$

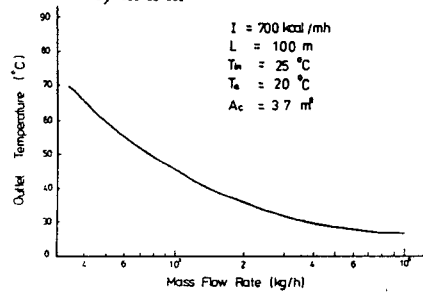


Fig. 4.5 Outlet temperature vs. mass flow rate (theoretical)

From these graphs a good fin efficiency was resulted when the fin thickness was over 1mm but less affected the outlet temperature. In this experiment the 10mm long and 0.8mm thick fin was used.

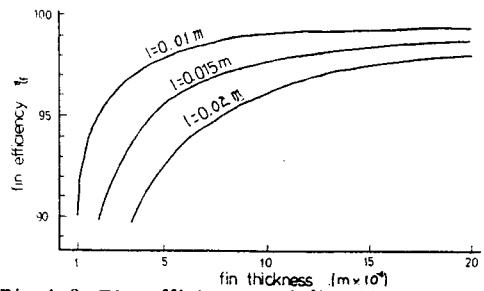


Fig 4.6 Fin efficiency and fin thickness

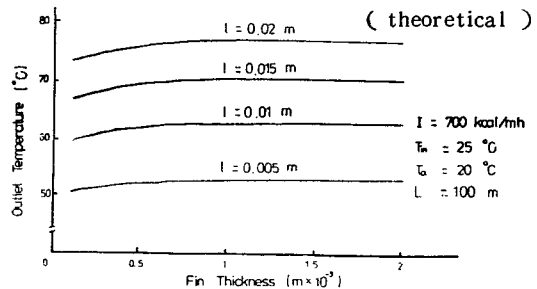


Fig.4.7 Relation between fin thickness(theoretical)

Fig 4-8 represents the experimental results of collector efficiencies with spine fin and without fin, and least squares line are fitted to the data.

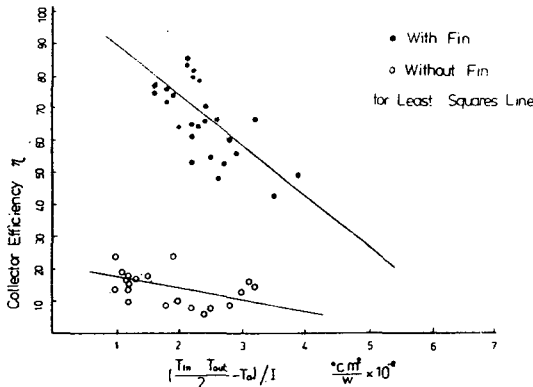


Fig. 4.8 Instantaneous efficiency of collector (experimental result)

From this figure one can see the collector efficiency of the former is higher about 4 to 5 times than the latter as expected naturally, while the efficiency decreasing rate vice versa.

The performance curves (3) and (4) of two collectors in this experiment were contrasted with those Utha university's (1) and (2) in Fig 4-9.

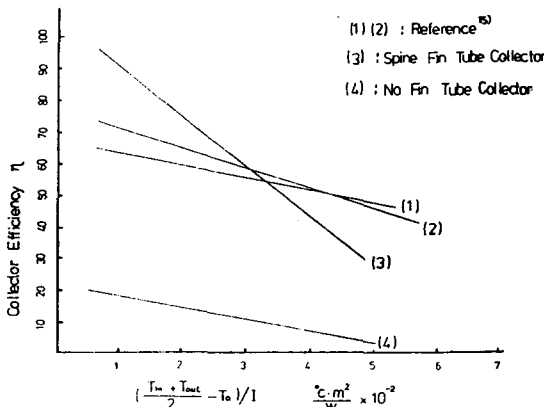


Fig. 4.9 Comparison of instantaneous with reference collector<sup>15)</sup>

Within the range of  $3 \times 10^{-2} \text{ } ^\circ\text{C m}^2 / \text{W}$  in X coordinate, collector (3) prevails in performance

over the collector (1) and (2).

More functionally, in turn, under  $60^\circ\text{C}$  of the outlet temperature collector (3) shows rather higher performance than the two collectors (1) and (2).

Though the two collectors specified here were not sufficient in fabrication and black paint surface treatment, these collectors showed a comparatively good results.

Using the specialized cover-glass and selective surface treatment, it is expected to be excellent performance for the spine fin tube solar collector.

## 5. Conclusions

Test have been performed on two solar collectors with and without spine fins to investigate the heat transfer characteristics through the experiment and theoretical analysis.

And obtained conclusions are as follow.

1) The outlet temperature of the solar collector with spine fins showed a good agreement when correction factor  $\gamma$  was 1.5 between the experimental and theoretical results.

2) Theoretically recommended optimum flow rate range is about  $0.2 \sim 1.4 \ell / \text{min m}^2$  in the spine fin tube solar collector when the temperature difference of the inlet and outlet were chosen about  $10^\circ\text{C}$  or more.

3) Fin efficiency was identified to increase linearly with the increase of fin thickness and fin length, but the former did not influence the outlet temperature to an appreciable extent when it was above 0.5 mm thick.

Thus the theoretical values of optimum range is recommended 10~15 mm long and

**References**

- 1) 横田理, 太陽エネルギーに対する平板集熱器の  
傳熱に関する研究, 冷凍 第52卷 595號,  
1977.5
- 2) 名工試 おける コレクタ-集熱特性 試験法  
名古屋 工業技術試験研究所報告 第26卷  
4號.
- 3) H.C. Hottel and B.B. Woerts, "The  
Performance of Flat Plate Solar Heat  
Collector" ASME Trans. Vol.64.1942.
- 4) G. Grossman, A. Shitzer and Y. Zvirn,  
"Heat Transfer Analysis of a Flat Plate  
Solar Energy Collector" Sol-Energy Vol  
19, No 5.
- 5) P.R. Smith and M.H. Cobble, "Numeri-  
cal Modeling of Flat Plate Solar Collector  
AIAA 10th Thermo Physics Conference,  
Denver, Colorado/May 27-29,1975.
- 6) John. A. Duffie, William A. Beckman,  
"Solar Engineering of Thermal Process"  
John Willey & Sons, Ins,1980,p201~214.
- 7) 太陽 Energy 利用技術開發 SERI -H-80-2  
韓國動力資源研究所.
- 8) J.P. Holman, "Heat Transter" 5th ed.